Development 126, 3703-3713 (1999)
Printed in Great Britain © The Company of Biologists Limited 1999
DEV6409



# Vegetal rotation, a new gastrulation movement involved in the internalization of the mesoderm and endoderm in *Xenopus*

**Rudolf Winklbauer* and Matthias Schürfeld**

Universität zu Köln, Zoologisches Institut, Weyertal 119, 50931 Köln, Germany
*Author for correspondence (e-mail: rwinkl@novell.biolan.uni-koeln.de)

*Accepted 28 May; published on WWW 19 July 1998*

## SUMMARY

**A main achievement of gastrulation is the movement of the endoderm and mesoderm from the surface of the embryo to the interior. Despite its fundamental importance, this internalization process is not well understood in amphibians. We show that in *Xenopus*, an active distortion of the vegetal cell mass, vegetal rotation, leads to a dramatic expansion of the blastocoel floor and a concomitant turning around of the marginal zone which constitutes the first and major step of mesoderm involution. This vigorous inward surging of the vegetal region into the blastocoel can be analyzed in explanted slices of the gastrula, and is apparently driven by cell rearrangement. Thus, the prospective endoderm, previously thought to be moved passively, provides the main driving force for the internalization of the mesendoderm during the first half of gastrulation. For further involution, and for normal positioning of the involuted mesoderm and its rapid advance toward the animal pole, fibronectin-independent interaction with the blastocoel roof is required**.

Key words: *Xenopus laevis*, Gastrulation, Involution, Mesoderm, Endoderm, Marginal zone, Cell intercalation, Morphogenesis

## INTRODUCTION

Gastrulation is the morphogenetic process by which, in metazoans, the germ layers are established in their characteristic spatial arrangement: ectoderm on the outside, endoderm inside, and mesoderm, if present, in between these two layers. Most often, the main activity of gastrulation involves the movement of the endoderm and mesoderm from the surface of the embryo to the interior, and a variety of mechanisms has developed in different groups of animals to achieve this internalization of germ layers.

Gastrulation movements have been extensively studied in amphibians, notably in *Xenopus*. In the amphibian blastula, the wall enclosing the blastocoel consists of a thin animal blastocoel roof (BCR) and a massive vegetal region. Most of the BCR will form ectoderm. During gastrulation, it spreads in the process of epiboly to eventually cover the embryo. The vegetal cell mass will contribute to the endoderm, and between vegetal region and BCR, in the marginal zone, mesoderm surrounds the embryo as a belt below the equator (Vogt, 1929; Keller, 1986). In *Xenopus*, the outer part of the dorsal marginal zone consists of prospective axial mesoderm, whereas the deep zone includes the head mesoderm. The endoderm extends into the marginal zone in the superficial layer, thus largely covering the mesoderm from the outside (Keller, 1975, 1976; Minsuk and Keller, 1997). Nevertheless, mesoderm is initially part of the blastocoel wall, and must be internalized during gastrulation together with the endoderm.

Despite the fundamental importance of this process, its mechanism is not well understood in *Xenopus*. Blastopore indentation at the vegetal boundary of the mesodermal belt is initiated by bottle cell formation, first dorsally and then laterally and ventrally (Hardin and Keller, 1988). However, the blastopore groove formed is shallow. Its deepening and the concomitant internalization of the mesoderm occur by involution: mesoderm and suprablastoporal endoderm roll over the blastopore lip, thereby turning inward. This is seen directly in time-lapse recordings (Keller, 1978), but is also evident from the fate map. In the early gastrula, more anterior mesoderm is located closer to the blastopore, more posterior mesoderm further animally, suggesting a rotation of the mesoderm in the course of gastrulation that inverts the anterior-posterior axis (Keller, 1976). It is generally assumed that the force for involution is provided by the mesoderm, whereas the mass of yolk-rich vegetal cells is internalized passively, e.g. by constricting the ring-like blastopore below the vegetal region. In fact, however, the driving force for mesendoderm internalization has not yet been localized experimentally. We show that contrary to previous belief, it is indeed an active movement of the vegetal cell mass that promotes initial mesoderm involution and the inward surging of prospective endoderm.

## MATERIALS AND METHODS

### Embryos and explants

*Xenopus laevis* embryos were obtained as described by Winklbauer (1990) and staged according to Nieuwkoop and Faber (1967). Techniques of operation and the buffer used (Modified Barth's Solution, MBS) have been described (Winklbauer, 1990).

### BCR-less embryos

At the earliest indication of pigment concentration at the future blastopore (stage 10 sharp), before formation of Brachet's cleft, the BCR was removed at the level of the blastocoel floor (BCF).

### Gastrula slices

From a stage 10 BCR-less embryo, a mid-sagittal slice about 5 cells thick was recovered which contained the dorsal blastopore. It was placed in MBS on a coverslip, which was sealed to the underside of a culture dish to cover a hole in the bottom of the dish. The slice was held flat by a strip of a second coverslip resting at its ends on silicon grease. The BCF of BCR-less embryos, slices, or slice fragments were recorded on video at epi-illumination in the time-lapse mode, or specimens were fixed in 4% formaldehyde in MBS.

### Labeling of donor embryos for grafting

Each blastomere of a 4-cell stage embryo was injected with 8 nl of 15-30 mg/ml Lucifer Yellow Dextran amine, $M_r$ $10\times10^3$. To visualize grafts, recipient embryos were fixed in 4% formaldehyde and fractured appropriately.

### Vital staining of the BCF

A few crumbs of Nile blue sulfate were dissolved in MBS in a small culture dish, such that BCR-less embryos just covered by the solution were still visible. After 3-5 minutes, embryos were washed briefly in MBS. Under these conditions, cut surfaces and the BCF are preferentially stained.

### Fibronectin (FN) peptide

HPLC-purified GRGDSP hexapeptide was from Novabiochem (Läufelfingen, Switzerland).

## RESULTS

### Dorsal mesoderm involutes mainly during the first half of gastrulation

Labeled homotopic grafts were used to follow the involution of the dorsal mesoderm. To determine the extent of this movement, outer marginal zone regions were transplanted at the initial gastrula stage, and host embryos were analyzed at the end of gastrulation (Fig. 1A-F). When the lower half of the blastopore lip adjacent to the bottle cells is transplanted (Fig. 1A), labeled cells appear over the anterior one third of the archenteron (Fig. 1B), the upper half of the lip (Fig. 1C) comes to overlie the posterior two thirds (Fig. 1D). Thus, as expected, all of the blastopore lip involutes. Elongation of involuted mesoderm due to spreading of anterior and convergent extension of axial mesoderm is evident. When the margin of the BCR directly above the lip is labeled (Fig. 1E), it is found to elongate in the outer layer of the embryo, as is typical of prospective neuroectoderm (Fig. 1F). This suggests that at the initial gastrula stage, the posterior limit of the dorsal mesoderm coincides with the border between lip region and BCR. Expression of *Xbra*, a marker indicating the posterior boundary of the mesoderm, substantiates this proposal (Ibrahim and R. W., unpublished data).

Involution movement was reconstructed from a series of

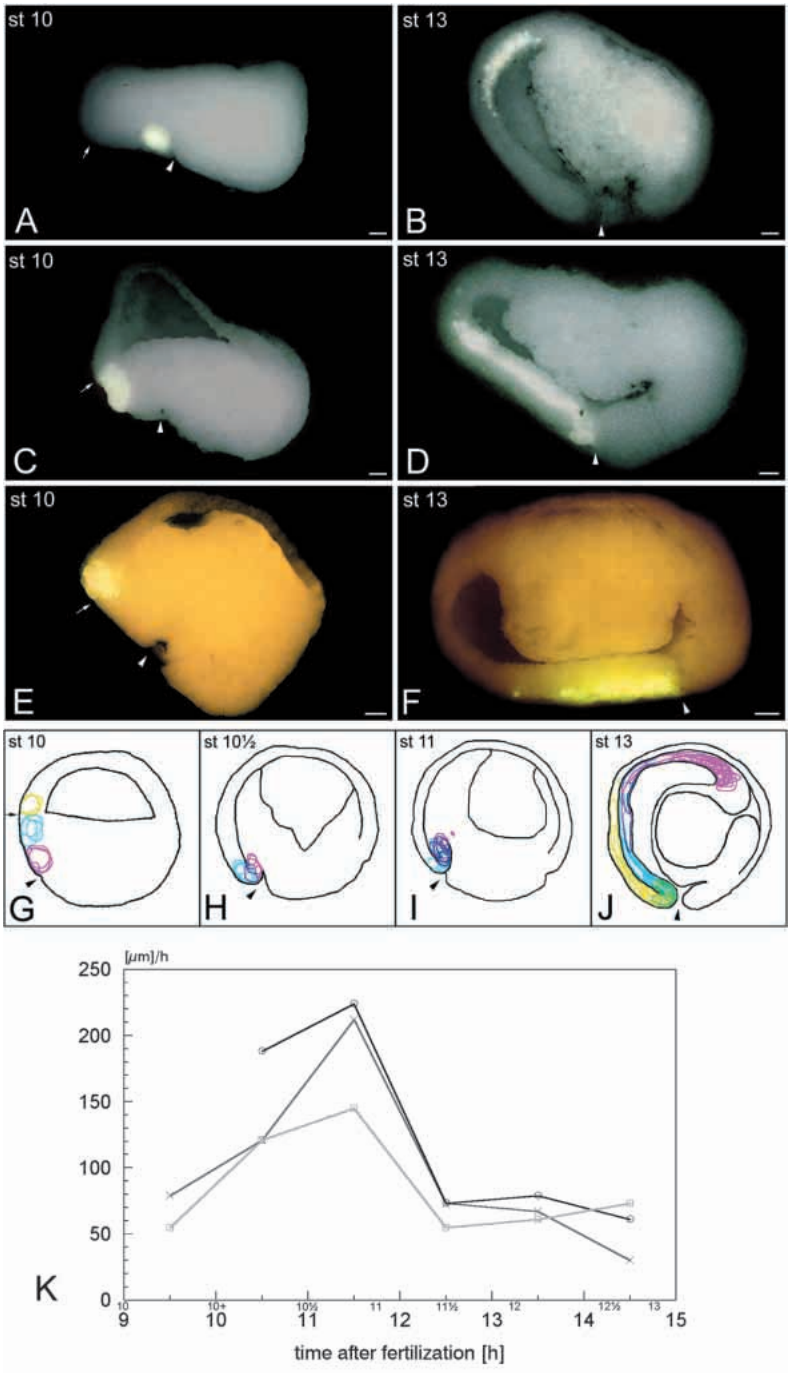


**Fig. 1.** Kinetics of dorsal mesoderm involution. Lower part of blastopore lip (A,B), upper part of lip (C,D) and margin of BCR (E,F) was labeled by homotopic transplantation of Lucifer Yellow Dextran-containing grafts at stage 10. Host embryos were fixed after 30 minutes (A,C,E) or at stage 13 (B,D,F). The dorsal blastopore is indicated by arrowheads. Bars, 100 µm. (G-J) Outlines ($n$=58) of dorsal lower lip (pink), upper lip (blue) and BCR margin grafts (yellow) implanted at stage 10 (G) and shown at subsequent stages (H-J). (K) Rate of involution movement. Distance to the blastopore of the remotest surface cells which disappeared at the lip within 1 hour were measured during consecutive intervals from time-lapse recordings of gastrulae. Each curve represents an embryo.

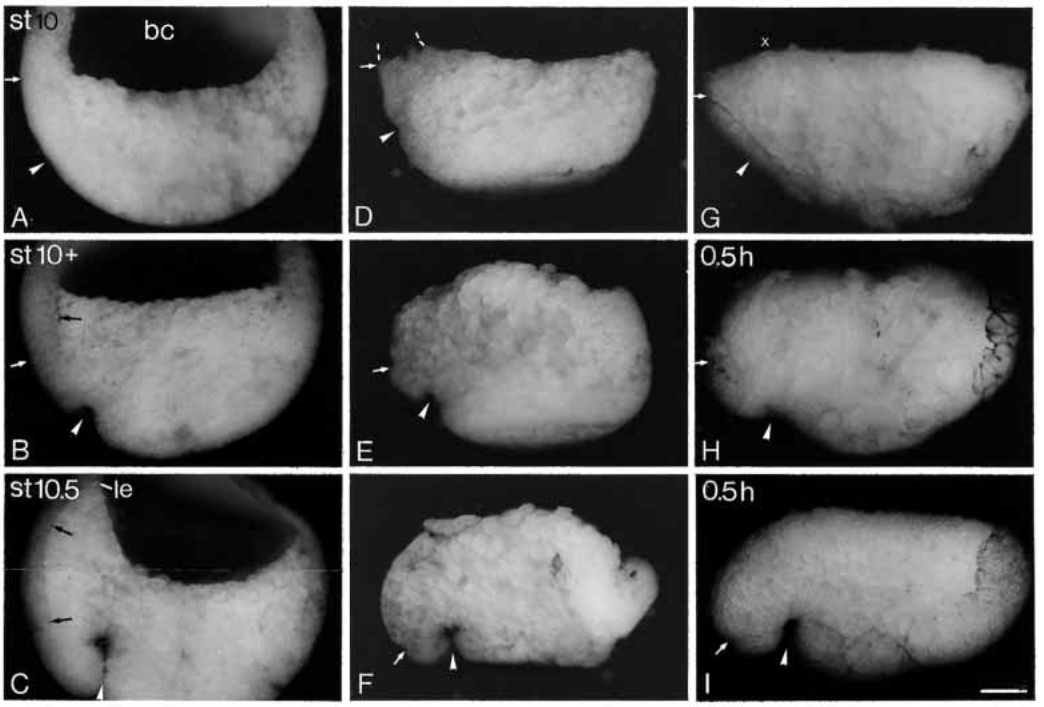


**Fig. 2.** Morphology of involution stages. Whole embryos (A-C), embryos from which the BCR had been removed at stage 10 (D-F), and mid-sagittal slices from stage 10 BCR-less embryos (G-I) were fixed at stages 10 (A,D,G), 10+ (B,E), 10.5 (C,F), or 0.5 hours after stage 10 (H,I), and fractured sagittally (A-F). Animal is to the top, dorsal to the left. The outer marginal zone is between the dorsal blastopore (arrowheads) and the boundary to BCR (white arrows). The dashed lines in D indicates the former position of BCR; black arrows, Brachet's cleft; X, bend of BCF; le, leading edge of mesendoderm; bc, blastocoel. Bar, 200 μm.

homotopic transplantations. In the initial gastrula, lower lip region, upper lip, and margin of the BCR are arranged in a vegetal to animal sequence (Fig. 1G). Two hours later, the upper lip region has moved vegetally and the lower half of the lip inward, the two regions lying now side by side (Fig. 1H). Another hour later, the former upper lip region has moved inward behind the previous lower lip (Fig. 1I). Thus, by a rapid rotation in the first half of gastrulation, the orientation of the outer marginal zone has become reversed. During the second half, all labeled regions elongate: the mesoderm inside the embryo and the neuroectoderm on the outside (Fig. 1J). That involution takes place mainly during the first half of gastrulation can be directly observed in the superficial layer of the marginal zone (Fig. 1K). The rate at which cells approach the dorsal blastopore lip increases to reach a maximum in the middle gastrula and it then falls abruptly to the initial low level.

### Rotation of the vegetal periphery initiates involution and formation of Brachet's Cleft

The initial stages of involution, as seen in sagittally fractured embryos, are shown in Fig. 2A-C. At stage 10, involution has not yet begun (Fig. 2A). One hour later (Fig. 2B), the blastopore invaginates dorsally and Brachet's cleft separates the leading edge mesoderm and endoderm from the BCR. The leading edge has not yet moved animally. A short cleft, but no blastopore, is visible on the ventral side. Another hour later, at stage 10.5 (Fig. 2C), the dorsal mesendoderm has advanced considerably to form a wall of cells applied to the BCR.

From whole embryo sections, it is not obvious whether Brachet's cleft forms by a local separation of inner and outer cells of the marginal zone, i.e. by delamination, or by moving the BCR downward over the mesoderm. Therefore, we examined embryos gastrulating after removal of the BCR. At stage 10, the small cells of the dorsal marginal zone extend far centrally at the BCF (Fig. 2D). After one hour, the outer marginal zone has begun to turn around the invaginating blastopore (Fig. 2E). A cleft of Brachet is not visible. Instead, the small-celled part of the BCF appears rotated outward by 90°, forming a vertical surface (above arrow) whose length is comparable to the length of Brachet's cleft in intact embryos. This suggests that the cleft is normally established by rolling the peripheral BCF against the BCR, i.e. by apposition, and not by delamination. Another hour later, the outer marginal zone has turned around the blastopore by 90° (Fig. 2F), which corresponds to the rotation observed in whole embryos (see Fig. 1).

Involution-related movements can also be examined in mid-sagittal slices of BCR-less embryos gastrulating between coverslips. A few minutes after explantation at stage 10 (Fig. 2G), the dorsal periphery has already started rotation, causing a bend in the BCF contour. 30 minutes later, blastopore invagination and rotation of the marginal zone have progressed to varying degrees (Fig. 2H,I), sometimes to a state attained in BCR-less embryos only after 2 hours (Fig. 2I, compare to Fig. 2F). Thus, movement in slices is 2-4 times faster than normal. Both in BCR-less embryos and in gastrula slices, rotation is initially restricted to the dorsal side. It starts ventrally with a 1- to 2-hour delay (Fig. 2F; not shown), as in the intact embryo, suggesting that the observed movements are not artificially provoked.

For further analysis, trajectories of cells were determined from time-lapse recordings of slices during consecutive intervals (Fig. 3). In the example shown, movement is under way when recording is started 10 minutes after operation at stage 10 (Fig. 3A). A persistent feature is the upwelling of the large-celled BCF. Since the lower surface of the vegetal region also shifts upward, the whole slice creeps in this direction (Fig. 3A-D). Marginally, movement is opposite. At the peripheral BCF, it is deflected outward, to pass into a strikingly rapid (up to 20 μm/minute) downward movement close to the surface of

the marginal zone. Vegetally, trajectories bend towards the blastopore. Since translocation is faster at the surface and slower toward the center, the region including the peripheral BCF and the marginal zone appears to rotate as a whole (Fig. 3A-D).

Although both the vegetal outer surface and the BCF shift upward, visible movement in the center of the vegetal region is slow, i.e. trajectories of fast moving cells end in or start from a region of low mobility, respectively (Fig. 3A-D). This may be due to movement of cells in the deeper layers of explants. In the upper part of the vegetal region close to the BCF, cells appear by intercalation from deep layers. Conversely, near the vegetal outer surface, cells disappear by moving to the interior (Fig. 3B). Thus, cell rearrangement and a corresponding movement of cells in the inner layers may account for the apparent discontinuity of visible movement in slices.

### Rotation of the vegetal periphery is associated with blastocoel floor spreading

The contour length of the BCF, as seen in fractured specimens, increases between stages 10 and 10.5 nearly twofold in BCR-less embryos, and about threefold in intact ones (see Fig. 2). Apparently, rotation of the vegetal periphery entails an expansion of the BCF area. In time lapse recordings of BCR-less embryos, this process can be studied (Fig. 4). At the beginning of gastrulation, centrifugal shifting of BCF cells starts dorsally (Fig. 4A). Movement increases on this side (Fig. 4B) and then expands laterally and ventrally (Fig. 4C), until at stage 10.5, most of the BCF is moving (Fig. 4D). Thus, centrifugal BCF movement spreads from dorsal to ventral during the first 2 hours of gastrulation. When the outer marginal zone is removed dorsally (Fig. 4E) or ventrally (Fig. 4F), BCF spreading is nevertheless initiated normally. No spreading, but contraction of the BCF occurs in late blastula BCR-less embryos (not shown).

As BCF cells move toward the margin, they are replaced by new cells emerging from deeper layers. In Fig. 4G, cells that appeared during the 30 minute interval represented in Fig. 4B are indicated. Evidently, intercalation is not restricted to the proximal rim of the outward moving zone, but is scattered all over it. Intercalation is to some extent countered by the disappearance of cells which move into deeper layers at the rim of the BCF (Fig. 4G). However, the rate of removal is only about half that of intercalation. In summary, BCF spreading can be accounted for by dispersed cell intercalation, which is not fully balanced by the disappearance of cells at the margin.

### The driving force for marginal zone rotation is generated in the vegetal cell mass

To identify the origin of the force for marginal zone rotation, gastrula slices were further dissected. First, slices were cut vertically at the level of the blastopore (Fig. 5A). The smaller explant consists essentially of marginal zone. It tends to round up immediately after cutting, but during recording, no significant movement occurs. In contrast, the complementary vegetal region fragment shows strong movement. The vegetal outer surface adjacent to the former blastopore bends upward, regardless of the presence or absence of residual bottle cells, and the upper part of the vegetal cell mass shifts animally. Also, cells disappear by moving into deeper layers close to the vegetal outer surface, and emerge from the deep layers close to the BCF. This is the same pattern as that observed in the vegetal cell mass of whole slices. However, at the cut margin, downward movement of cells occurs in a region which normally shows upward translocation. This rapid outward and downward movement reconstitutes the translocation pattern of complete slices at a more central position. Together, movement in the two complementary fragments suggests that the force driving marginal zone rotation may be generated in the vegetal cell mass.

When cut half-way between the blastopore and the center of a slice, motion is concentrated in the fragment containing the periphery of the vegetal mass together with the marginal zone (Fig. 5B). It consists again of a downward translocation in the

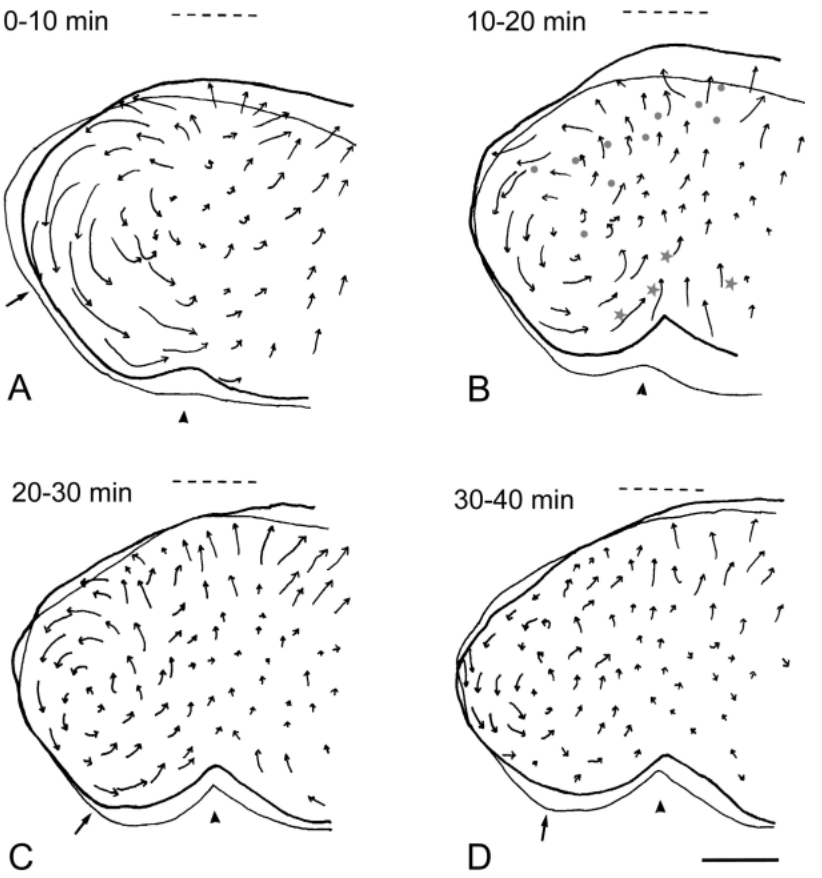


**Fig. 3.** Movement in gastrula slices. (A-D) Trajectories of cells in a mid-sagittal slice from a stage 10 BCR-less embryo. In B, positions of disappearing cells (grey stars) and cells appearing at the surface (grey dots) are indicated. The slice moves upward, with the BCF approaching the dashed reference line. Initial (thin outline) and final position (thick outline) are shown for each interval. Blastopore (arrowheads) and the site where the BCR had been attached (arrows) delimit the outer marginal zone. Dorsal is to the left, animal to the top. Bar, 100 μm.

vegetal cell mass close to the cut margin, in about the same region as in Fig. 5A. However, movement is clockwise instead of counter-clockwise. The larger fragment containing the central vegetal region shows the same pattern of trajectories as the corresponding fragment in Fig. 5A, but downward movement is slower and occurs at a still more central position (Fig. 5B). Overall, it appears that rapid downward movement can be induced within the vegetal cell mass by vertical cuts. To see how far this propensity extends, slices were bisected medially, and the cut margin of the ventral half was observed (Fig. 5C). The vegetal outer surface does not shift upward, and only a few isolated cells rush downward at the margin. Thus, downward movement is induced most strongly at the periphery of the vegetal cell mass.

A strip of peripheral vegetal mass (Fig. 5D) does indeed perform pronounced movements, and all elements of the translocation pattern of slices can be recognized: upward motion in the lower and upper part, a low mobility zone, and rapid outward and downward movement at lateral margins (Fig. 5D). Isolated upper and lower halves show movements typical of the respective regions of whole such explants (Fig. 5G). An adjacent, more central strip (Fig. 5E) displays the same pattern, but translocation is less pronounced. In contrast, a fragment from the ventral half shows mostly weak, irregular movement (Fig. 5F). Apparently, movement in fragments is not a non-specific effect of cutting, but reveals a distinct pattern of motility in the vegetal region. The results suggest that rotation of the periphery as a whole is due to active movement within the vegetal cell mass – vegetal rotation – which drives passive rotation, or involution, of the marginal zone.

## Normal mesoderm positioning requires interaction with the BCR

During the first 2 hours of gastrulation, the outer marginal zone is rotated by 90°, and this movement occurs also in BCR-less

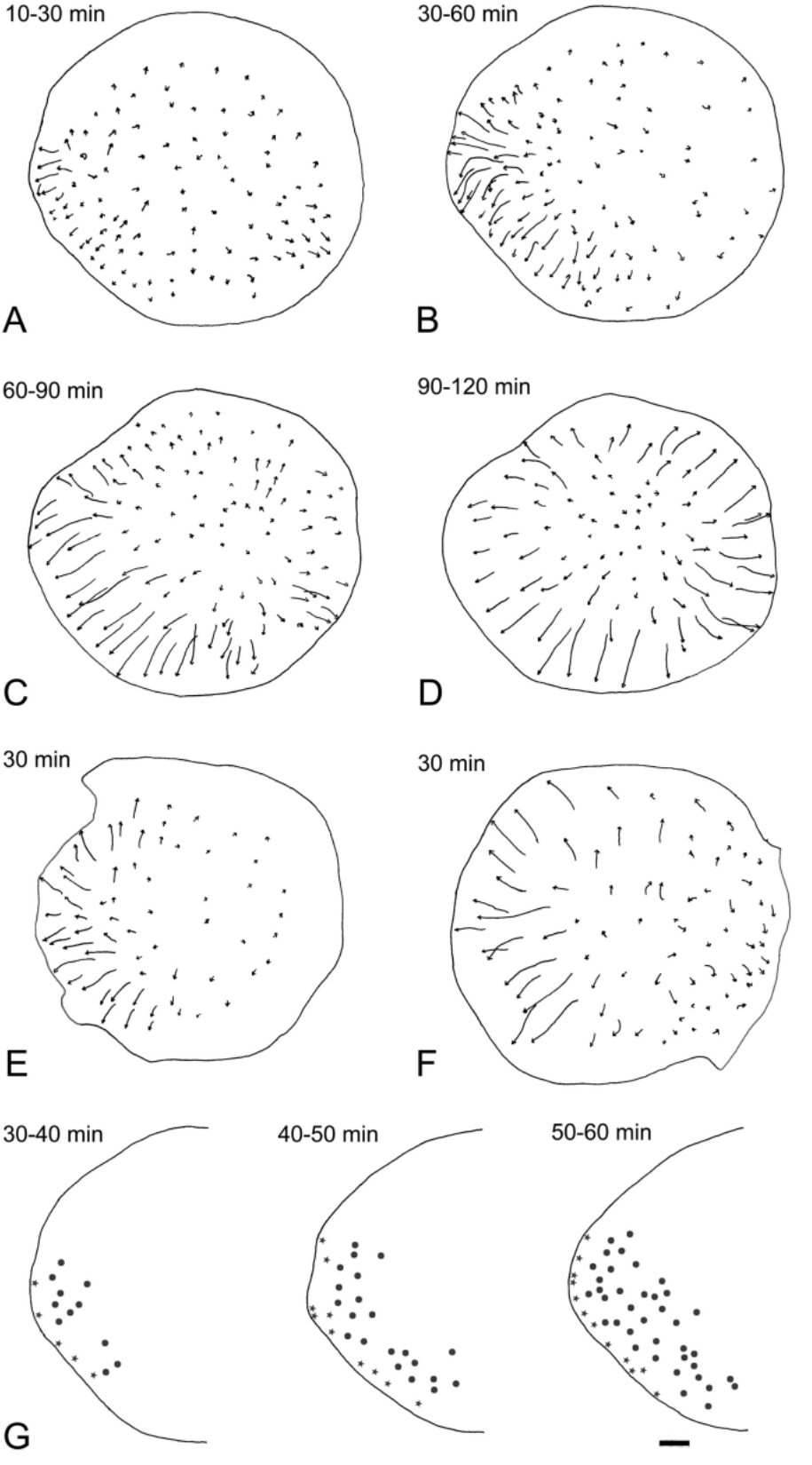


**Fig. 4.** Blastocoel floor spreading.
(A-D) Trajectories of BCF cells. Recording was started 10 minutes after removal of the BCR at stage 10, time intervals are indicated. The arrow-free region at the margin (A,B) corresponds to the rapidly contracting cut surface where the BCR had been attached. (E,F) BCF movement during the first 30 minutes of recording, BCR and dorsal (E) or ventral (F) marginal zone were removed at stage 10. (G) Interval shown in B, resolved into 10 minute intervals. Cells appear by intercalation (grey dots) or disappear in the deeper layers (grey stars). In the 50- to 60-minute interval, cells begin to disappear also by moving beyond the edge of the explant, due to the rotation of the periphery (not shown). Dorsal is to the left; bar, 100 μm.

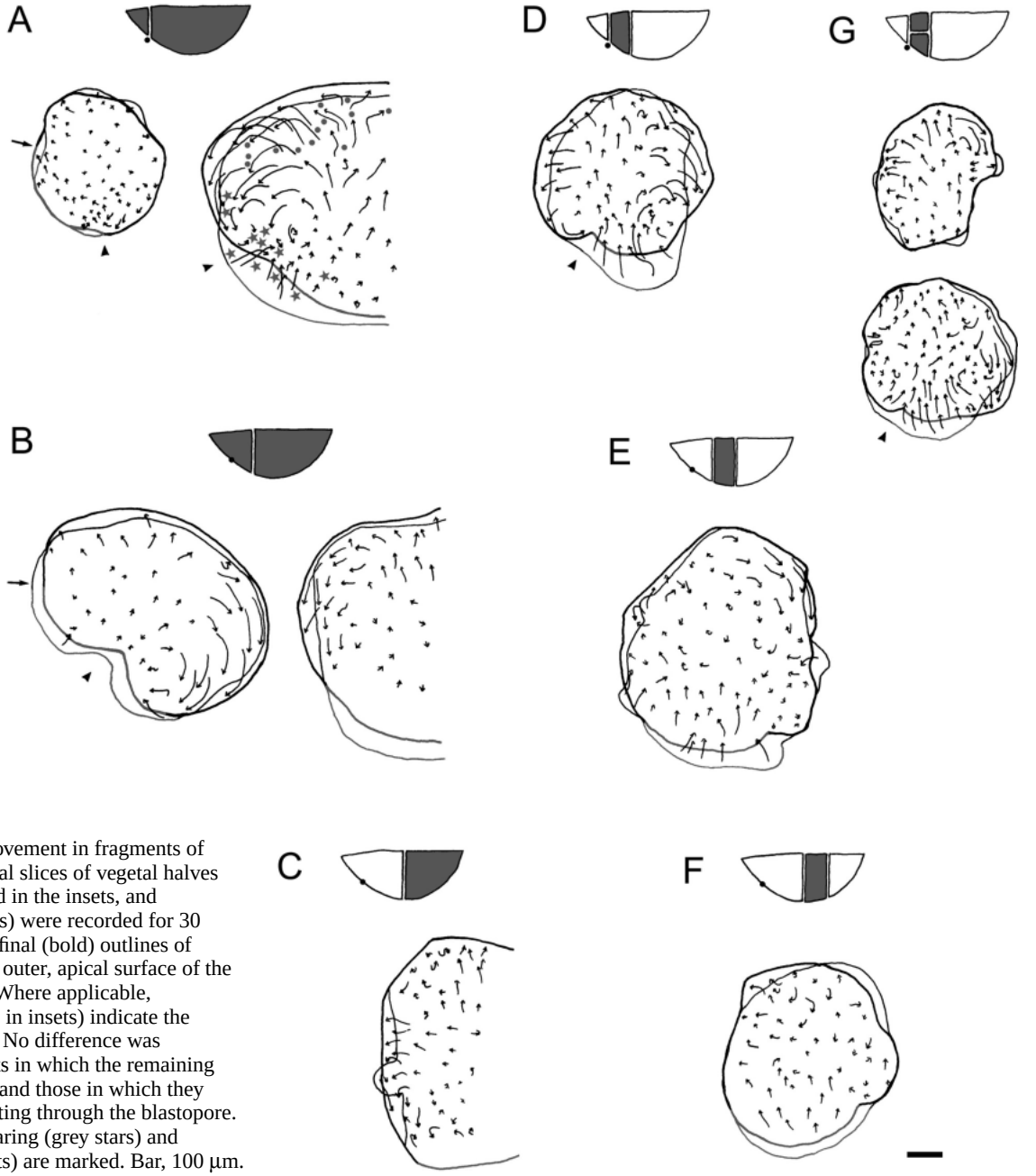


**Fig. 5.** Vegetal rotation movement in fragments of slices. Stage 10 mid-sagittal slices of vegetal halves were dissected as indicated in the insets, and fragments (shaded in insets) were recorded for 30 minutes. Initial (thin) and final (bold) outlines of explants are indicated; the outer, apical surface of the embryo is shown in grey. Where applicable, arrowheads (or black dots, in insets) indicate the position of the blastopore. No difference was observed, between explants in which the remaining bottle cells were removed and those in which they were left in place after cutting through the blastopore. In A, positions of disappearing (grey stars) and reappearing cells (grey dots) are marked. Bar, 100 μm.

embryos or in gastrula slices (see Figs 1, 2). During the next hour, inversion of the outer marginal zone is completed in the embryo, and the archenteron elongates (Figs 1, 6A). In BCR-less embryos, the archenteron also lengthens dramatically during that time, to nearly penetrate the BCF (Fig. 6B). However, the prospective mesoderm is not properly allocated. It forms a compact mass, instead of a layer which extends animally beyond the archenteron tip. Presence of the BCR may be required for the mesoderm to assume its characteristic shape and position.

When a third of the BCR is left on the dorsal side of otherwise BCR-less embryos, a normal mesoderm layer forms between archenteron and BCR (Fig. 6C). This could be a mechanical effect of the BCR remnant, which is stabilized against outward bending by being attached laterally as well as dorsally to the lower half of the embryo. When rolled against it, the mesendoderm could be squeezed upward. However, a reasonable mesoderm layer also forms with a narrow flap of BCR. Since it is not attached laterally, it could easily be bent and moved downward by the rotating marginal zone, but instead, it tends to spread animally together with the underlying mesoderm (Fig. 6D). Apparently, the effect of the BCR is not purely mechanical. An important component of the BCR is a matrix of FN fibrils which promotes mesoderm adhesion and migration. Interaction with the FN matrix is inhibited by RGD peptide (Winklbauer and Keller, 1996). Nevertheless, in the presence of the peptide, mesoderm layer formation is normal in embryos with the dorsal third of the BCR (Fig. 6E), although in controls, mesoderm cell spreading on FN was inhibited (not shown). Thus, some FN-independent interaction with the BCR is required for normal mesoderm positioning.

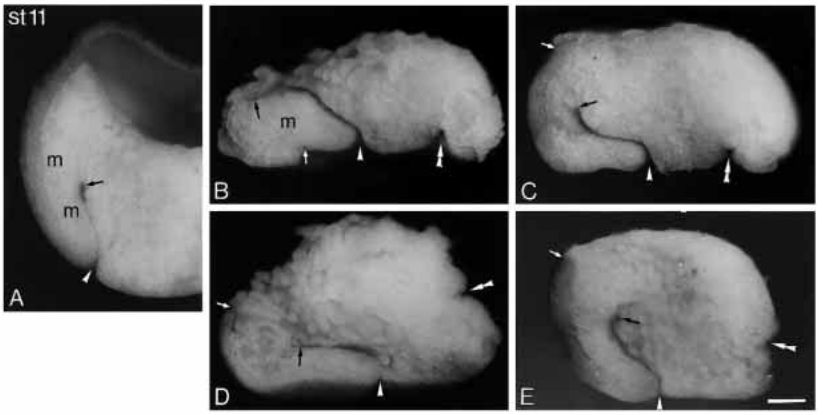


**Fig. 6.** BCF interaction with the BCR. Whole embryos (A), embryos with BCR completely removed at stage 10 (B), with the BCR removed except for the dorsal one third (C,E) or except for a narrow dorsal flap of BCR (D) were fixed at stage 11 and fractured sagittally. Some embryos with partially removed BCR were cultured in 4 mg/ml of GRGDSP peptide from stage 10 onwards (E). Animal is to the top, dorsal (arrowheads) and ventral blastopore (double arrowheads), cut margin of the BCR (white arrows), and anterior end of archenteron (black arrows) and position of mesoderm (m) are indicated. Bar, 200 μm.

For further analysis, the dynamics of the BCF was visualized by labeling its cells in the living condition. Short submersion of stage 10 BCR-less embryos in nile blue sulfate solution stains the superficial layer of BCF cells. Within minutes after staining, intercalating unlabeled cells appear (Fig. 7A). After 1 hour, most labeled cells have moved to the margin to accumulate in a narrow ring (Fig. 7B). This is also seen in fractured specimens fixed after 2 hours (Fig. 7C), and is consistent with BCF cell behavior as revealed in time-lapse recordings (Fig. 4G).

When some BCR is left dorsally, it apposes to the outward rotating, stained BCF. In the area of contact, intercalation of non-labeled cells is absent or reduced even after 2 hours, and centrifugal movement of cells is abrogated (Fig. 7D). Also, when a patch of BCR from an unstained embryo is applied to labeled dorsal BCF, intercalation is blocked in this area (Fig. 7E). However, when BCR is left in contact with the BCF for 3 hours, to stage 11, unlabeled cells appear in a broad zone behind the stained cells (Fig. 7F). Apparently, these are freshly involuted cells which spread on the BCR, the labeled, BCR-stabilized region being displaced animally.

This localized insertion of cells 2 hours after the onset of gastrulation does not occur in the absence of BCR interaction. When BCR-less embryos are labeled 2 hours after stage 10, some intercalation still occurs during the next hour on the central BCF (Fig. 7G), but not in the dorsal, rotated part which is now stable without BCR contact. However, unlabeled cells are not inserted above the blastopore (Fig. 7H). Also, when BCR is

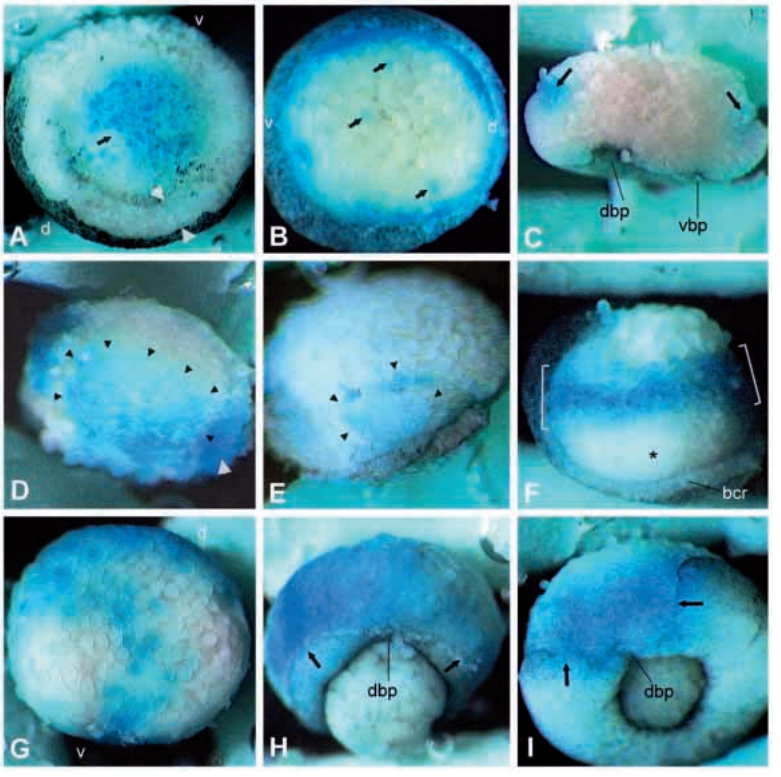


**Fig. 7.** Effects of the BCR on BCF dynamics. (A-C) Stage 10 embryos devoid of the upper part of the BCR were submersed in nile blue solution. After staining, the remaining BCR was removed. (A) When observed immediately, the cut surface where BCR had been attached appears white (between arrowheads), the BCF blue, intercalation is under way dorsally (arrow). (B) After 1 hour, the cut surface has contracted, and most, but not all (arrows) labeled cells are in a ring at the margin. (C) This ring (arrows) is also visible in fractured embryos after 2 hours. (D) BCF was stained at stage 10, BCR applying to the BCF was left on the dorsal side for 2 hours, and was then removed. Former area of contact between BCR and BCF stains blue (arrowheads). Intercalation occurred in the BCF outside this area (white region above). Laterally, labeled cells accumulated at the margin (white arrowhead). (E) A BCR-less embryo was stained at stage 10, a patch of BCR from an unstained embryo was applied to the BCF, and removed after 2 hours. Former position of the patch is indicated by arrowheads. Dorsal view. (F) Same experiment as in D, but with the dorsal BCR removed later, after 3 hours. A zone of non-labeled cells (asterisk) is inserted between labeled cells (between brackets) and the blastopore below the remnants of the dorsal BCR (bcr). Intercalation of white cells occurs also above the labeled zone, where BCF had not been in contact with BCR. (G,H) The BCR was removed at stage 10, embryos were cultured for 2 hours, stained, and cultured for another hour. Animal view (G) and dorsovegetal view (H) of same embryo. Cut margins of BCR are indicated (arrows). (I) BCR was removed dorsally 2 hours after the start of gastrulation, embryos were stained and cultured for an additional hour. No insertion of cells takes place above the dorsal blastopore. Each experiment involving 3-5 embryos was repeated 2-4 times. d, dorsal; v, ventral; dbp, dorsal blastopore; vbp, ventral blastopore.

removed dorsally 2 hours after the onset of gastrulation, to stain the BCF including the BCR-apposed side of the advancing mesoderm, no insertion of cells is observed during the following hour (Fig. 7I).

### Rapid translocation of internalized mesoderm and endoderm

Rotational apposition of the BCF to the BCR, and the substratum-dependent insertion of cells may both contribute to the animally directed movement of the involuted mesendoderm. Its translocation was quantified by measuring the advance of its leading edge relative to the blastopore, with epibolic shifting of the latter subtracted, in two batches of embryos (Fig. 8). Displacement of the dorsal leading edge starts one hour after blastopore formation (Fig. 8A,B). The edge advances first at 6-12 μm/minute, and then more gradually, to eventually reach rates of up to 27 μm/minute. This is significantly faster than migration of single mesoderm cells or explants in vitro (1-3 μm/minute) (Winklbauer, 1990; Winklbauer and Nagel, 1991), but is comparable to velocities attained in vegetal rotation movements. The ventral leading edge shows little translocation when epiboly is subtracted (Fig. 9A,B). Lengthening of the dorsal archenteron parallels the advance of the leading edge only roughly. The distance between archenteron tip and leading edge increases initially, and diminishes continually in the second half of gastrulation (Fig. 9C,D). Apparently, the tip moves forward relative to the anterior mesendoderm.

## DISCUSSION

### Vegetal rotation, a morphogenetic process driving initial mesoderm and endoderm internalization

Among invertebrates, vegetal cells may vary greatly in size and number, but they always arrange in a single epithelial-like layer. Its inpocketing, i.e. gastrulation by invagination, is a common way to internalize the endoderm and associated mesoderm (e.g. Fioroni, 1987). Primarily holoblastic vertebrates are unique in developing a multilayered vegetal cell mass as a result of cleavage, and gastrulation movements may have become adapted to this. In fact, the amphibian vegetal endoderm does not exhibit classical invagination. However, our results show that in *Xenopus*, the vegetal cell mass is

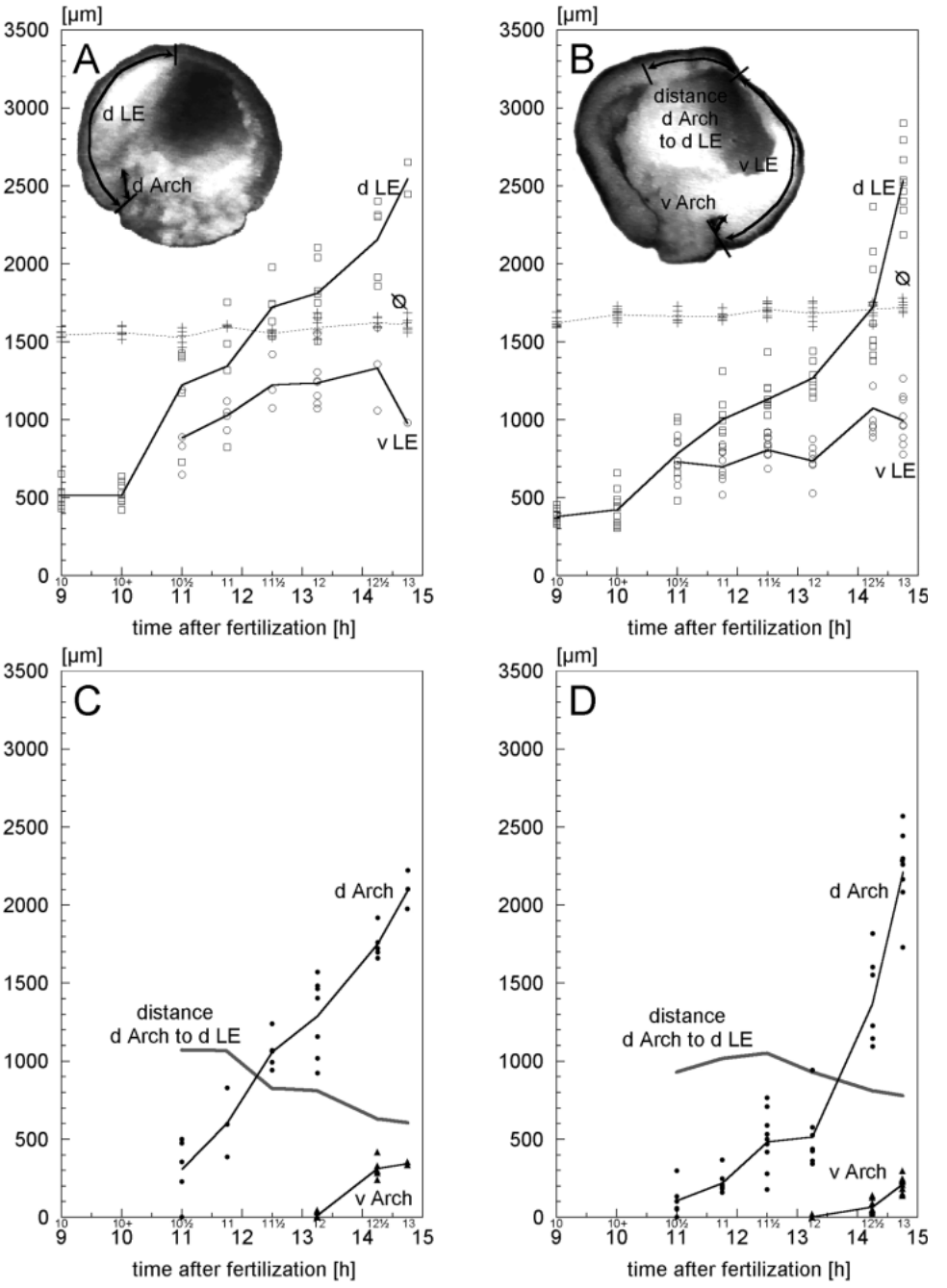


**Fig. 8.** Translocation of internalized mesendoderm. Distance between blastopore and dorsal leading edge (dLE, open squares), ventral leading edge (vLE, open circles), anterior tip of dorsal archenteron (dArch, dots) and ventral archenteron tip (vArch, triangles) was measured in two batches of embryos (A,C and B,D) of about equal diameter (dotted lines; crosses) after fixation and mid-sagittal fracturing. Lines of measurement are indicated in the insets (A,B). Epibolic displacement of blastopore (2.0 μm/minute dorsally, 1.7 μm/minute ventrally) was independently determined from video recordings of embryos and subtracted. Each symbol (square, circle etc.) represents a measurement on a single embryo, lines connect the average values of the parameters, respectively. Average values for the distance between dorsal archenteron tip and leading edge, from the same embryos, are shown (C,D).

nevertheless morphogenetically active and dominates the initial phase of mesendoderm internalization.

Overall, the respective movement is an inward surging of the vegetal mass into the blastocoel. In contrast to invagination, the vegetal outer surface does not contract and pocket in as a whole. Instead, movement is concentrated at the periphery: narrowing of the vegetal cell mass occurs by bending upward its lower part near the blastopore. At the same time, the upper part of the vegetal region expands, and the marginal zone is rotated downward. Thus, the actual inpocketing of the embryonic surface is restricted to a submarginal annulus, with the inner lining of the blastopore groove being formed by the locally bent vegetal surface, the outer one by the rotated marginal zone, and the hinge region by the bottle cells (Fig. 9).

Narrowing of the lower and the concomitant expansion of the upper vegetal region is an active process, whereas rotation of the marginal zone is passive and a consequence of the first movement. The main evidence for this notion is that autonomous, sustained distortion movements occur only in slice fragments that contain a sufficient amount of vegetal cell mass. These distinctly patterned, reproducible movements differ from healing reactions, i.e. the rounding up of explants to minimize cut surfaces, as seen e.g. in vegetal halves and slices before the onset of gastrulation (unpublished results). The active process is best described as a rotation of the peripheral vegetal cell mass in the radial plane, that furthermore progresses from dorsal to ventral roughly in parallel to blastopore formation. If this vegetal rotation movement is derived from mesendodermal invagination of invertebrates, it has been substantially modified.

Vegetal rotation is independent of bottle cells. Movement in explants occurs equally well in their presence or absence, and when gastrula slices are cultured to the stage where involution begins ventrally, vegetal rotation is seen to preceed bottle cell formation at this side (unpublished results). This explains why mesoderm involution is initiated even when the prospective bottle cells are removed before their apical contraction (Keller, 1981).

In the virtual absence of cell shape changes, active rearrangement of vegetal cells would be expected to drive rotation. Since distortions proceed in thin tissue slices, force-generating cell movements should be oriented radially within the vegetal mass, not circumferentially. Unfortunately, the in vivo pattern of rearrangement is not known. From the trajectories of cells, one must conclude that movement deep within a slice is different from that on its surface, to account for continuity of translocation through a zone of apparent low mobility. Surface movement may be aberrant due to exposure of cells normally in contact with others, and to friction generated at the coverslip. Therefore, the inferred pattern of translocation in the deep layers of slices may be representative of normal vegetal cell movement.

Since cells approach the low mobility zone vegetally and leave it animally, the inferred deep layer movement is also from vegetal to animal. Actually, a simple interpretation of our findings would be that vegetal cells are all crawling animally, using surrounding cells as substrata (Fig. 9). If mobility decreased towards the BCF, more vegetal cells would crawl between the slower cells ahead, thus expanding the BCF by intercalation. Appropriate gradation of velocities, probably also along the radial dimension, would produce the observed tissue distortions. If active migration were impeded in cells exposed to the surface, cells at the cut margins of slice fragments would be moved downward by more interior cells struggling to crawl upward, which agrees with observation. Finally, oriented creeping of slices or fragments is also consistent with cells crawling animally. Vegetal cells form lamellipodia and filopodia in vitro (Wacker et al., 1998), but are also able to move by cortical tractoring in the absence of cytoplasmic processes (Kubota, 1981).

Vegetal rotation ceases at the same endpoint both in BCR-less embryos and in gastrula slices. Movement in slices is much faster, but stops correspondingly sooner. After 1 hour, the most advanced specimens have not progressed beyond a stage reached after 30 minutes (unpublished results). This corresponds, however, to the stage 2 hours after operation where BCF spreading diminishes dorsally in BCR-less embryos. Apparently, not the duration but the extent of movement is predetermined. The force driving rotation may also be preset, the actual velocity of movement being determined by the load imposed. As vegetal rotation spreads from dorsal to ventral, the moving region is always in lateral contact to the non-rotating cell mass, which may attenuate movement. Also, by rotating as a torus that surrounds the vegetal core, the tissue has to be expanded where it moves outward, and be compressed at the opposite movement. Gastrula slices would be released from such loads, and could show correspondingly faster rotation.

### Substratum dependence of mesoderm layer formation

In BCR-less embryos, vigorous expansion of the central BCF is associated with a contraction of the peripheral area that normally would develop into the substratum side of the advancing mesendoderm. Interaction with the BCR suffices to prevent this idling motion. Instead of accumulating in a compact mass at the former margin of the BCF, the mesoderm forms an extended layer along the BCR. Several processes seem to be involved in this substratum-dependent behavior of the involuted mesoderm.

The anterior *cerberus* (*cer*) domain (see below) is stabilized by the BCR. Intercalation is diminished, and the attached BCF area is prevented from being pushed toward the margin by ongoing intercalation in the remaining BCF. Whether the *cer* domain actually extends anteroposteriorly at later stages, as suggested by the inferred shape changes depicted in Fig. 9, has yet to be demonstrated. Behind the *cer* region, interaction with the BCR permits the insertion of cells into the substratum-apposed surface (Fig. 9). From its position, it should be mainly the *gsc* domain that appears to spread on the BCR. As it extends anteroposteriorly, it flattens against the BCR, such that it occupies a larger part of the mesendodermal surface. Shape changes of the *goosecoid* (*gsc*)-expressing region during gastrulation (Vodicka and Gerhart, 1995) are consistent with this notion.

Insertion of the *gsc* domain (see below) is substratum dependent, but it is not clear whether extension itself, or only the alignment of extension with the substratum requires BCR contact. In favor of the second possibility, the supposed cell rearrangement in the extending *gsc* domain corresponds to a radial intercalation movement, and this can proceed substratum independently in open-faced explants of dorsal mesoderm

(Wilson and Keller, 1991). As indicated in Fig. 9, it could drive the lowering of the lip region. Part of the *gsc* domain should be present in the above Keller explants, and extension of this domain in the embryo could be a local expression of the radial intercalation movement seen in explants. Also, the archenteron lengthens in BCR-less embryos, probably by being attached to a *gsc* domain that extends independently of a substratum. However, the domain may lose contact to the surface under these circumstances, and sink into the mesendodermal cell mass. The function of the BCR would be to keep the *gsc* domain at the surface of the mesoderm, and to direct extension properly. However, we cannot exclude at present that substratum-dependent extension of the *gsc* domain, and perhaps also of the more anterior *cer* domain, is a novel process not related to radial intercalation as observed in Keller explants.

## Reconstruction of mesoderm internalization movements

We combined fate map and marker gene expression data to define subregions of the dorsal mesoderm (Fig. 9A). In the initial gastrula, an outer marginal zone containing prospective axial/paraxial mesoderm, and a deep zone which includes the head mesoderm, can be distinguished (Keller, 1976). The panmesodermal marker *eomesodermin* (*eomes*) is expressed in both regions. A posterior subregion of the *eomes* domain, largely corresponding to the axial/paraxial mesoderm, is defined by the expression of *Xbra* (Ryan et al., 1996). On the dorsal side, *Xbra* expression does not extend into the BCR (Ibrahim and R. W., unpublished data), and the limit of mesoderm involution coincides with the boundary between blastopore lip region and the BCR (this article). Vegetal and interior to the *Xbra* domain, the *goosecoid* (*gsc*)-expressing region (De Robertis et al., 1992; Vodicka and Gerhart, 1995; Artinger et al., 1997) comprises the prospective head mesoderm (Keller, 1976).

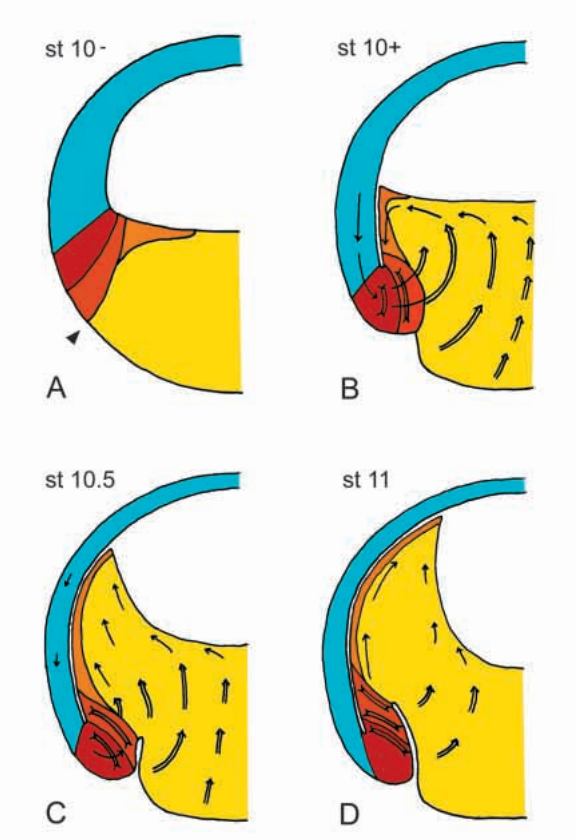


**Fig. 9.** Reconstruction of involution movements. Schematic drawings of stage 10– (A), stage 10+ (B), stage 10.5 (C) and stage 11 (D) dorsal gastrula halves. Yellow, prospective vegetal endoderm; orange, *cer*-expressing region; dark orange, *gsc* domain; red, *Xbra* domain; blue, prospective ectoderm of the BCR. Double arrows, active vegetal rotation movement; inverted double arrows, active radial intercalation; arrows, passive movement. Arrowhead, site of blastopore formation. For simplicity, suprablastoporal endoderm is omitted.

The *Xbra* and *gsc* domains together do not exhaust the *eomes* domain. A region is left at the peripheral BCF which will be located most anteriorly after the start of involution. As judged from its supposed later position, it corresponds to the *cerberus* (*cer*) expressing region. Large yolky cells of the leading edge are eventually found in the liver primordium, which suggested that *cer* may be expressed in prospective endoderm (Bouwmeester et al., 1996). However, we consistently observed that a layer of small cells, also apparent in histological sections (e.g. Hausen and Riebesell, 1991), extends up to the leading edge and separates the large endodermal cells from the BCR. Being located in front of the *gsc* domain, it should move beyond the anterior end of the embryo to the ventral side (Keller, 1976). Cells behaving like this have recently been described as expressing *Xaml* and being destined to participate in blood formation, suggesting a mesodermal affiliation (Tracey et al., 1998). Thus, we tentatively include the small-celled region that coexpresses *eomes* and *cer* in the mesoderm. In following the regions thus defined through gastrulation, we recognize three phases of internalization.

*1. Stage 10 to 10.5.* The first 2 hours of gastrulation are dominated by active vegetal rotation. It leads to a passive rotation of the outer marginal zone, which constitutes the initiation of mesoderm involution, and interiorly to the apposition of BCF to the BCR. In the first half of this period (Fig. 9B), the BCR seems to move downward together with the BCF rolled against it. In this way, Brachet's cleft is established without an advance of the leading edge towards the animal pole. As reported previously (Nieuwkoop and Florschütz, 1950), the cleft forms occasionally before the blastopore has appeared. Together with our finding that the margin of the dorsal BCR represents prospective neuroectoderm, this suggests that vertical contact between components of neural induction may be established at earliest gastrula stages. At stage 10+, BCF apposition already extends up to the posterior part of the prospective forebrain (Poznanski and Keller, 1997).

During the second half of this phase (Fig. 9C), a rising wall of mesodermal and endodermal cells forms. We propose that this is due to continued BCF apposition, but in the absence of further strong downward shifting of the BCR. Constraining cell mobility in the BCF area rolled against the BCR, but continuing intercalation in the remaining BCF, may effectively transform downward rotation of the vegetal periphery into the rapid building-up of a wall of cells at the BCR.

This process corresponds to an advance of the leading edge which should be independent from cell migration. Anterior mesoderm cells which contact the BCR are migratory and form locomotory protrusions in an FN-dependent manner (Winklbauer, 1990; Winklbauer and Keller, 1996). However, advance of the leading edge (Nakatsuji, 1975; this article) is

much faster than the velocity of mesoderm cells or explants crawling in vitro (Winklbauer, 1990; Winklbauer and Nagel, 1991; Wacker et al., 1998). Moreover, blocking migration by inhibiting interaction with the FN matrix of the BCR does not prevent normal positioning of the mesoderm in whole embryos (Winklbauer and Keller, 1996) or in partially BCR-less ones (this article). This suggests that migration is not crucial for the initial advance of the mesendoderm on the BCR. At any rate, the *cer*-expressing domain becomes localized during this phase to the leading edge of the mesendodermal cell mass.

*2. Stage 10.5-11.* At least in vitro, dorsal vegetal rotation seems to cease during this period, but at the same time, externally visible involution movement is most rapid. Two processes may replace vegetal rotation as the motive force for involution, and complete rapid internalization. First, behind the *cer* domain, the *gsc* region spreads along the BCR, which would tend to pull the *Xbra* domain inward (Fig. 9D). Second, the vegetal alignment zone is established as an arc across the preinvolution part of the dorsal lip region. Beneath the outer surface, cells begin to exhibit mediolateral intercalation behavior, in a position where the hoop stress thus generated would tend to snap the *Xbra* domain downward and inward (Lane and Keller, 1997). Both processes may cooperate to bring the *Xbra* domain into its definitive position.

Like vegetal rotation and BCF apposition at early, and convergent extension at later stages, extension of the *gsc* domain along the substratum, by some kind of radial intercalation, should contribute to moving the mesoderm forward. Driving mesoderm translocation largely by cell rearrangements may render *Xenopus* gastrulation rather insensitive to perturbation of cell crawling on the FN matrix. Moreover, at rearrangement, small and slow changes in individual cell positions are summed up into rapid large-scale movements, explaining why mesoderm translocation in the embryo can be several times faster than its velocity of migration.

*3. Stage 11-13.* At stage 11, the mesoderm has attained its definitive anterior-posterior arrangement (Fig. 9D), and during the second half of gastrulation, the posterior boundary of the *Xbra* domain does not change noticeably (Ibrahim and R. W., unpublished). However, as the *Xbra*-expressing circumblastoporal collar constricts to eventually close the blastopore, its volume must decrease proportionally. We propose that, at a given cross section, cells leaving the collar to the interior are constantly replaced by cells that move in from laterally, due to contraction of the collar. In this way, the *Xbra* domain can maintain its shape and relative position despite the continuation of involution at a slow pace. Circumferential constriction at the outer side of the blastopore lip, due to mediolateral intercalation behavior that has spread posteriorly, could drive this involution at later stages of gastrulation (Keller et al., 1992).

We thank Ray Keller for discussions, advice on terminology, and numerous suggestions to improve the manuscript, and Stephan Wacker, Hady Ibrahim and Martina Nagel for discussions and help with the figures. This work was supported by the DFG.

## REFERENCES

**Artinger, M., Blitz, I., Inoue, K. Tran, U. and Cho, K. W. Y.** (1997). Interaction of *goosecoid* and *brachyury* in Xenopus mesoderm patterning. *Mech. Dev.* **65**, 187-196.

**Bouwmeester, T., Kim, S.-H., Sasai, Y., Lu, B. and De Robertis, E. M.** (1996). Cerberus is a head-inducing secreted factor expressed in the anterior endoderm of Spemann's organizer. *Nature* **382**, 595-601.

**De Robertis, E. M., Blum, M., Niehrs, C. and Steinbeisser, H**. (1992). Goosecoid and the organizer. *Development* **Supplement** 1677-171.

**Fioroni, P.** (1987). *Allgemeine und Vergleichende Embryologie der Tiere.* Berlin, Heidelberg, New York: Springer.

**Hardin, J. and Keller, R.** (1988). The behaviour and function of bottle cells during gastrulation of *Xenopus laevis. Development* **103**, 211-230.

**Hausen, P. and Riebesell, M.** (1991). *The Early Development of Xenopus laevis.* Berlin, Heidelberg, New York: Springer.

**Keller, R. E.** (1975). Vital dye mapping of the gastrula and neurula of Xenopus laevis. I. Prospective areas and morphogenetic movements of the superficial layer. *Dev. Biol.* **42**, 222-241.

**Keller, R. E.** (1976). Vital dye mapping of the gastrula and neurula of Xenopus laevis. II. Prospective areas and morphogenetic movements of the deep layer. *Dev. Biol.* **51**, 118-137.

**Keller, R. E.** (1978). Time-lapse cinemicrographic analysis of superficial cell behavior during and prior to gastrulation in *Xenopus laevis. J. Morph.* **157**, 223-248.

**Keller, R. E.** (1981). An experimental analysis of the role of bottle cells and the deep marginal zone in gastrulation of *Xenopus laevis*. *J. Exp. Zool.* **216**, 81-101.

**Keller, R. E.** (1986). The cellular basis of amphibian gastrulation. In *Developmental Biology: A Comprehensive Synthesis Vol. 2: The Cellular Basis of Morphogenesis* (ed. L. Browder), pp. 241-327. New York: Plenum.

**Keller, R., Shih, J. and Domingo, C.** (1992). The patterning and functioning of protrusive activity during convergence and extension of the *Xenopus* organizer. *Development 1992* **Supplement,** 81-91.

**Kubota, H. Y.** (1981). Creeping locomotion of the endodermal cells dissociated from gastrulae of the Japanese newt, *Cynops pyrrhogaster*. *Exp. Cell Res.* **133**, 137-148.

**Lane, M.C. and Keller, R.** (1997). Microtubule disruption reveals that Spemann's organizer is subdivided into two domains by the vegetal alignment zone. *Development* **124**, 895-906.

**Minsuk, S. B. and Keller, R. E.** (1997). Surface mesoderm in Xenopus: a revision of the stage 10 fate map. *Dev. Genes Evol.* **207**, 389-401.

**Nakatsuji, N.** (1975). Studies on the gastrulation of amphibian embryos: Cell movement during gastrulation in Xenopus laevis embryos. *Wilhelm Roux' Arch. dev. Biol.* **178**, 1-14.

**Nieuwkoop, P. D. and Florschütz, P. A.** (1950). Quelques caractères spéciaux de la gastrulation et de la neurulation de l'oeuf de *Xenopus laevis*, Daud. et de quelques autres anoures. 1ère partie. Étude descriptive. *Arch. Biol.* **61**, 113-150.

**Nieuwkoop, P. D. and Faber, J.** (1967). *Normal Table of Xenopus laevis (Daudin).* North-Holland, Amsterdam.

**Poznanski, A. and Keller, R.** (1997). The role of planar and early vertical signaling in patterning the expression of Hoxb-1 in Xenopus. *Dev. Biol.* **184**, 351-366.

**Ryan, K., Garrett, N., Mitchell, A. and Gurdon, J. B.** (1996). *Eomesodermin*, a key early gene in Xenopus mesoderm differentiation. *Cell* **87**, 989-1000.

**Tracey Jr, W. D., Pepling, M. E., Horb, M. E., Thomsen, G. H. and Gergen, J. P.** (1998). A *Xenopus* homologue of *aml-1* reveals unexpected patterning mechanisms leading to the formation of embryonic blood. *Development* **125**, 1371-1380.

**Vodicka, M. A. and Gerhart, J. C.** (1995). Blastomere derivation and domains of gene expression in the Spemann organizer of X*enopus laevis*. *Development* **121**, 3505-3518.

**Vogt, W.** (1929). Gestaltungsanalyse am Amphibienkeim mit örtlicher Vitalfärbung. II. Teil. Gastrulation und Mesodermbildung bei Urodelen und Anuren. *Wilhelm Roux' Arch. dev. Biol.* **120**, 384-706.

**Wacker, S., Brodbeck, A., Lemaire, P., Niehrs, C. and Winklbauer, R.** (1998). Patterns and control of cell motility in the *Xenopus* gastrula. *Development* **125**, 1931-1942.

**Wilson, P. and Keller, R.** (1991). Cell rearrangement during gastrulation of *Xenopus*: direct observation of cultured explants. *Development* **112**, 289-300.

**Winklbauer, R.** (1990). Mesodermal cell migration during Xenopus gastrulation. *Dev. Biol.* **142**, 155-168.

**Winklbauer, R. and Nagel, M.** (1991). Directional mesodermal cell migration in the Xenopus gastrula. *Dev. Biol.* **148**, 573-589.

**Winklbauer, R. and Keller, R.** (1996). Fibronectin, mesoderm migration, and gastrulation in Xenopus. *Dev. Biol.* **177**, 413-426.